Journal of Polymers and the Environment (2021) 29:3756–3769
https://doi.org/10.1007/s10924-021-02148-9

ORIGINAL PAPER

Gelatin Beads/Hemp Hurd as pH Sensitive Devices for Delivery of Eugenol as Green Pesticide

Gianluca Viscusi[1] · **Giuliana Gorrasi**[1]

Accepted: 12 April 2021 / Published online: 22 April 2021

Abstract

In this paper gelatin beads reinforced with natural hemp hurd have been produced as pH sensitive devices for the release of eugenol, as green pesticide. The composites beads, with a mean diameter of about 1 mm, were obtained by polymer droplet gelation in sunflower oil. Thermal properties were evaluated showing no noticeable difference after the introduction of hemp hurd. Barrier properties demonstrated an improvement of hydrophobization. The introduction of 5% w/w of hemp hurd led to a reduction of sorption coefficient of about 85% compared to unloaded gelatin beads. Besides, the diffusion coefficient decreased, introducing 5% w/w of hemp hurd, from 8.91×10^{-7} to 0.77×10^{-7} cm^2/s. Swelling and dissolution phenomena of gelatin beads were studied as function of pH. The swelling of gelatin beads raised as pH increased up to 2.3 g/g, 9.1 g/g and 27.33 g/g at pH 3, 7 and 12, respectively. The dissolution rate changed from 0.034 at pH 3 to 0.077 h^{-1} at pH 12. Release kinetics of eugenol at different pH conditions were studied. The released eugenol after 24 h is 98%, 91%, 81 and 63% w/w (pH 3), 87%, 62%, 37 and 32 wt% (pH 7) and 81%, 68%, 60 and 52 wt% (pH 12) for unloaded gelatin beads and gelatin beads with 1%, 3 and 5% of hemp hurd, respectively. The eugenol release behavior was demonstrated to be highly sensitive to the pH release medium, which allows to tune such devices as green pesticide release systems in soils with different level of acidity/basicity.

Keywords Green pesticides · Hemp hurds · Biocomposite · Eugenol · Release

Introduction

Nowadays, with the emerging intensification of farming systems, higher production and increased efficiency are required. In fact, some agricultural products are sold off season; that is greatly due to the excessive use or misuse of synthetic pesticides [1]. In the last 50 years, the average yields of some product crops are increased as pesticide use increased, even for controlling the deterioration due to insect pests [2]. Although these benefits as well as the economical relevance are noticeable, the intensive use of them is leading to serious environmental issues [3] as well as to ill effects on benign insects [4] In general, a synthetic pesticide is defined as a substance able to repel, reduce, destroy or kill unwanted organism such as pests. Some of them, called persistent pesticides, are substances that tend to accumulate in the environment with a half-life ranging between 5 and 15 years [5, 6]. As a consequence, the increase in pollution risk is being verified [7–9] meanwhile the adverse effects of synthetic pesticides have been found out regarding either the human health [10, 11] or the environment [12, 13]. This is even due to the fact that, according to some estimations, roughly 0.1% of used product reaches the target; the residual 99.9% tends to enter the environment [2, 14]. However, the misuse of synthetic pesticides over a long period can not only be a source of harmful effect to soil, animals and humans but along with that, it could lead to a series of side effects such as the possibility for some pests to resist to them, the growth of stronger pests, the possibility to attack not targeted organisms, the too high concentration of pesticides in food products. To sum up, the not controlled use of pesticides could seriously be a source of hazardous effects on environment posing a threat to ecosystem [15–17]. All these unspeakable considerations are requiring, nowadays, a green and innovative alternative to protect crops without generating harmful consequences on ecosystem [1, 18]. A possible route lies in the use of natural derived substances

✉ Giuliana Gorrasi
ggorrasi@unisa.it

[1] Department of Industrial Engineering, University of Salerno, via Giovanni Paolo II, 132, 84084 Fisciano, SA, Italy

(in general from plants, seeds, roots, leaves etc.) able to be effective against pests as well as to be safer than synthetic pesticides [19]. These substances could act as insecticides, antifeedants, insects-growth regulators and repellent, representing a valid green alternative to synthetic pesticides. From practical point of view, the dispersion of pesticides in the soil is a crucial issue [17]. Except from volatilization, the retention on soil particles and degradation biotic and abiotic are the most noteworthy processes that could control the fate of pesticides. Both processes could lead to either transitory or permanent accumulation of pesticides in the soil. To avoid that, the use of new approaches is required aiming of guaranteeing a controlled dispersion of green pesticides in soil [20, 21]. Controlled release methodologies are emerging as a versatile tool to avoid or reduce such problems [22]. Among various strategies adopted, encapsulation is taking a center stage as a technique to achieve a controlled release device. In this process, an active compound is usually encapsulated in the biopolymer hydrogel which acts as a slow or safe release carrier of insecticide. Usually, biodegradable polymeric matrices such as cellulose, agarose, starch, chitosan gelatin or albumin are employed [23–26]. Scientific literature reports many pesticide controlled release systems such as calcium alginate-starch microspheres for the release of chlorpyriphos [27], ethyl cellulose incorporating clay and nanoclays loaded with atrazine [28], ethyl cellulose polymer microspheres for controlled release of norfluazon [29], alginate-gelatin beads crosslinked by $CaCl_2$ encapsulating cypermethrin [30], sodium alginate-poly (vinyl alcohol) system for base-triggered release of dinotefuran [31] and many other systems [32, 33]. Among the different preparation techniques, the polymer droplet gelation could represent an innovative approach to process a soil-compatible and bio-based polymer matrix such as Gelatin (Ge). It is a natural water-soluble protein obtained from collagen [34] characterized by biodegradability, low cost, abundancy and renewability [35–38]. In the attempt to improve the physical properties of polymeric beads, to control the release rate of the loaded green pesticide and safely protect it from degradation phenomena in the soil, lignocellulosic biomass can be incorporated into the polymeric matrix. Lignocellulosic biomass derived from fiber-based plants is being taken into consideration as scientific and technological innovation in the area of new materials [39] since they have properties such as low cost, low density, biodegradability, recyclability, specific mechanical properties, and flexibility in processing [40–43]. Its use could represent an environmentally friendly choice [24, 25]. Based on the above, this research focuses on the design and the preparation of an innovative green composite made up of hemp hurds reinforcing gelatin beads as a pH-sensitive delivery system of an active compound. Thermal, barrier and swelling properties of the polymeric composite beads were analyzed. Since the pH-triggered beads have been attracting increasing interest, the effect of pH level of the release medium and hemp hurd concentration were studied on either the release rate of the green pesticide or the swelling behavior of composite hydrogels. Results of the present investigation highlight the potentiality of novel gelatin/hemp hurd biocomposites as pH sensitive release systems of eugenol, as green pesticide. To the best of authors' knowledge no scientific papers are still reported on the formulated biocomposites.

Experimental

Materials

Hemp hurds (HH) were supplied by Nafco Company (Naples). Gelatin from bovine skin (CAS: 9000-70-8) was purchased from Sigma Aldrich in powder form. Eugenol (CAS: 97-53-0) was purchased from Sigma Aldrich. Sunflower oil (Selex) was purchased in a local market. Finally, NaOH in pellet form (CAS: 1310-73-2) was purchased from Sigma Aldrich while HCl solution 37% v/v (CAS: 7647-01-0) was purchased from Carlo Erba Reagents.

Beads Preparation

Prior to perform droplet gelation process, hemp hurds have been grinded using a stainless stell blade grinder (Duronic-CG250). The reduction in size is required to better disperse the lignocellulosic matrix inside the polymeric matrix. The hemp hurd grinded (HH) was sieved using a aluminium sieve with mesh size of 250 µm. Gelatin (Ge; 1.6 g), Eugenol (Eu; 10 wt% on gelatin basis) and HH (1%, 3 and 5% on polymer basis) were mixed with 15 mL of water and stirred at 45 °C for 4 h. The solution was added dropwise to sunflower oil kept at 4 °C using ice bath. To complete gelification, the beaker containing the oil and the prepared beads was kept in an ice water mixture for 2 h. Then, gelatin beads were collected from the dispersed phase and washed several times with pure ethanol and distilled water to obtain the Ge–Eu-HH-x (x= wt% of hemp hurd powder) composite beads. Finally, the composite beads were air dried for 48 h. Figure 1 reports a schematization of the gelification process and, by way of example, the picture of Ge–Eu-HH 1% beads was also reported.

Methods

Beads diameter was evaluated by analyzing digital images. To ensure statistical representativeness, 50 gelatin beads were analyzed for each condition. The bead diameters were obtained from recorded photographs and are expressed as the mean ± standard deviation. The mean value of bead diameter was

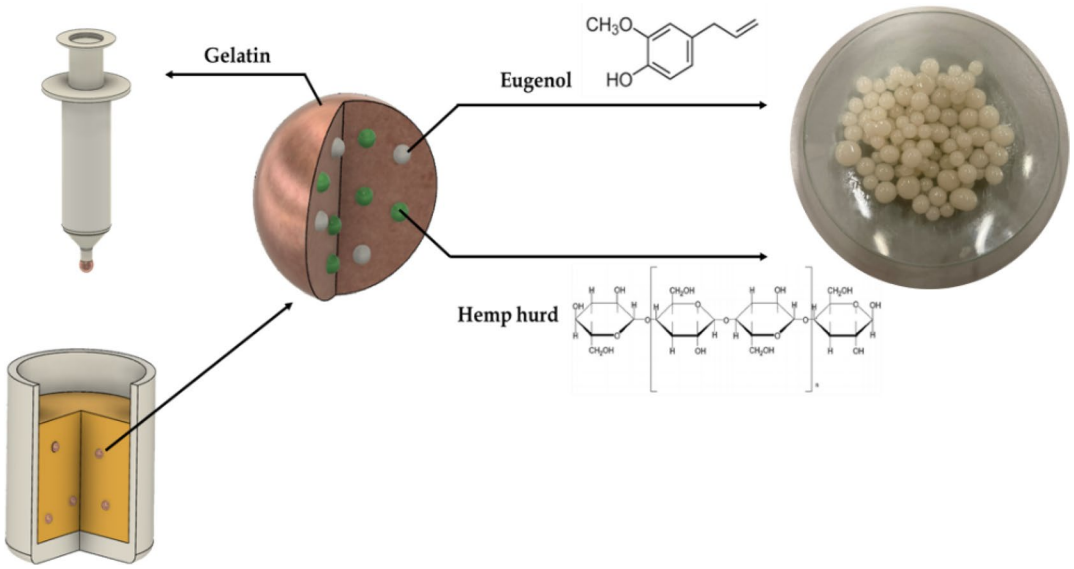

Fig. 1 Schematization of gelification process

hereainafter used for applying the mathematical modeling of the release kinetics.

Thermogravimetric analyses (TGA) were carried out in an air atmosphere for evaluating the thermal stability of hydrogel composites and the effect of hemp hurd on it. A Mettler TC-10 thermobalance from 30 to 400 °C at a heating rate of 10 °C/min was used.

Differential scanning calorimetry (DSC) were carried out for evaluating the effect of hemp hurd on melting temperatures of hydrogel composites. A thermal analyzer Mettler DSC 822/400 under N_2 atmosphere from 25 to 250 °C at a heating rate of 10 °C/min was used.

Barrier properties to water vapor were evaluated using a DVS Automated multi-vapor gravimetric sorption analyzer, using dry nitrogen as a carrier gas, to investigate the water adsorption properties of produced composites. The temperature was fixed to 30 °C. Samples were exposed to increasing water vapor pressures obtaining different water activities a%P/P_0 (from a%0.1 to a%0.8), where P_0 is the saturation water pressure at the experimental temperature. The adsorbed water mass was measured by a microbalance and recorded as a function of time. Measuring the variation of weight of the sample as a function of time, at a given partial pressure, it was possible to obtain the equilibrium value of sorbed vapor, C_{eq} ($g_{solvent}/g_{dry\ basis}$). In order to analyze the sorption isotherms, the Sips model was adopted [44, 45]. Being a combination of Langmuir and Freundlich isotherms and it is given the following general expression (Eq. 1):

$$q_e = \frac{q_m \times a_s c_{eq}^{1/n}}{1 + a_s c_{eq}^{1/n}} \tag{1}$$

where *qe* is the is amount of the adsorbate at equilibrium (mg/g), $_{eq}$ is equilibrium water concentration of the adsorbate on the adsorbent, q_m is the monolayer adsorption capacity (mg/g), is Sips isotherm model constant and *n* il related to the heterogeneity of the system.

Swelling properties of gelatin beads were determined since they are supposed to affect the relase rate of a delivery system. Firstly, 10 mg of material were air-dried and then weighed. Then, they were immersed in 20 mL of liquid medium (pH 3, pH 7 and pH 12) solution for different periods of time. The pH values of the tested release media were adjusted at 3 and 12 using 0.1 M HCl and 0.1 M NaOH solutions, respectively. Wet samples were wiped with filter paper to remove excess liquid and weighed. The swelling degree (SD) was calculated as (Eq. 2):

$$SD(\%) = \frac{W_w - W_{dry}}{W_{dry}} \times 100 \tag{2}$$

where W_w and W_{dry} are the weights of the beads measured at a specific time point and the initial weight of air-dried samples. A Voight-based equation (Eq. 3) has been applied to describe the experimental swelling data [46]:

$$S_t = S_{eq}(1 - e^{-t/r}) \tag{3}$$

where S_t is the swelling at time t, S_{eq} is the equilibrium swelling, τ is a rate constant.

Dissolution kinetics were determined, as for swelling properties, to better understand the release behavior of composite hydrogels. As first step, gelatin beads were dried for 24 h in a vacuum oven. The dry matter (M_0)

was weighed and immersed in 15 mL of liquid medium at different pH values (3, 7 and 12), kept under mechanical stirring. At fixed time intervals, the beads were taken out, dried under vacuum conditions and the weight was recorded. The solubility kinetic, for each pH value, was determined by plotting the gelatin beads weight as a function of the dissolution time. For each sample, tests were performed in triplicate, and average value was recorded. Equation 4 was proposed to describe the dissolution kinetics of gelatin beads:

$$m(t) = M_{\max} \times \exp(-k_{pH} \times (t - t^*)) \tag{4}$$

where M_{max} represent the maximum weight of Ge beads reached at stationary phase and t × represent the time corresponding to the stationary phase.

The release kinetics of eugenol were performed by ultraviolet spectrometric measurement using a Spectrometer UV-2401 PC Shimadzu (Japan). The tests were performed using a fixed amount of composite beads (200 mg), placed into 15 mL of ethanol and stirred at 100 rpm in an orbital shaker (VDRL MOD. 711%+%Asal S.r.l.). The release medium was withdrawn at fixed time intervals and replenished with fresh medium. The considered band was at 280 nm. The effect of pH and hemp hurd concentration on release kinetics were taken into account. The experimental data were fitted according to Baker and Lonsdale model (Eq. 5) [47].

$$\frac{3}{2} \times \left\{ 1 - \left(1 - \frac{M_t}{M_\infty} \right)^{2/3} \right\} \times \frac{M_t}{M_\infty} = k \frac{t}{r^2} \tag{5}$$

where M_t is the amount of drug released at time t, $M\infty$ is the amount of drug release at infinite time, k is the Baker-Lonsdale release constant and r is the radius bead, supposing it to have spherical shape [48]. Since the gelatin beads underwent to swelling phenomena, which are differently affected by pH level of release medium, the bead radius is supposed to be time-dependent (r%r(t)). Equation 6, obtained from Eq. 3 by expliciting the definition of Swelling degree (S_t), needs to be considered for the time interval from 0 to 24 h (maximum time before prevalence of dissolution phenomena):

$$m(t) = M_0 \times \left[1 + S_{eq} \left(1 - e^{-t/\tau} \right) \right] \tag{6}$$

after 24 h, the dissolution phenomena are supposed to occur and the bead mass underwent a reduction. Then, at times higher than 24 h, the Eq. 4 will be considered to describe the mass variation of gelatin beads.

For a spherical bead, considering the equation of a spherical volume, the time-dependent radius equations were derived. Equation 5 could then be modified by substituting the radius r on the right side of the equation with the previously obtained time-dependent radius equations and embedding all the constant parameters in the k' and k'' coefficients. The time-dependent radius equation are reported as Eqs. 7 and 8:

$$0 < t < 24h \frac{3}{2} \times \left\{ 1 - \left(1 - \frac{M_t}{M_\infty} \right)^{2/3} \right\} \times \frac{M_t}{M_\infty} = k' \frac{t}{\left[M_{0\times} \left(1 + S_{eq} (1 - e^{-t/\tau}) \right) \right]^{\frac{2}{3}}} \tag{7}$$

$$t > 24h \frac{3}{2} \times \left\{ 1 - \left(1 - \frac{M_t}{M_\infty} \right)^{2/3} \right\} \times \frac{M_t}{M_\infty} = k'' \frac{t}{\left[M_{\max} \times \exp(-k_{pH} \times (t - t^*)) \right]^{\frac{2}{3}}} \tag{8}$$

Table 1 k' and k'' parameters obtained from fitting of experimental data applying Eqs. 7 and 8

Sample	pH 3		pH 7		pH 12	
	k ($g^{2/3} \times h-1$)	k'' $^{2/3} \times h^{-1}$)	k' ($g^{2/3} \times h^{-1}$)	k'' ($g^{2/3} \times h^{-1}$)	k' ($g^{2/3} \times h^{-1}$)	k'' ($g^{2/3} \times h^{-1}$)
Ge–Eu	0.0342	0.0047	0.0190	0.0039	0.0028	0.0016
Ge-HH-Eu 1%	0.0263	0.0035	0.0062	0.0033	0.0013	0.0015
Ge-HH-Eu 3%	0.0132	0.0028	0.0044	0.0026	0.0011	0.0011
Ge-HH-Eu 5%	0.0091	0.0022	0.0031	0.0014	0.0006	0.0006

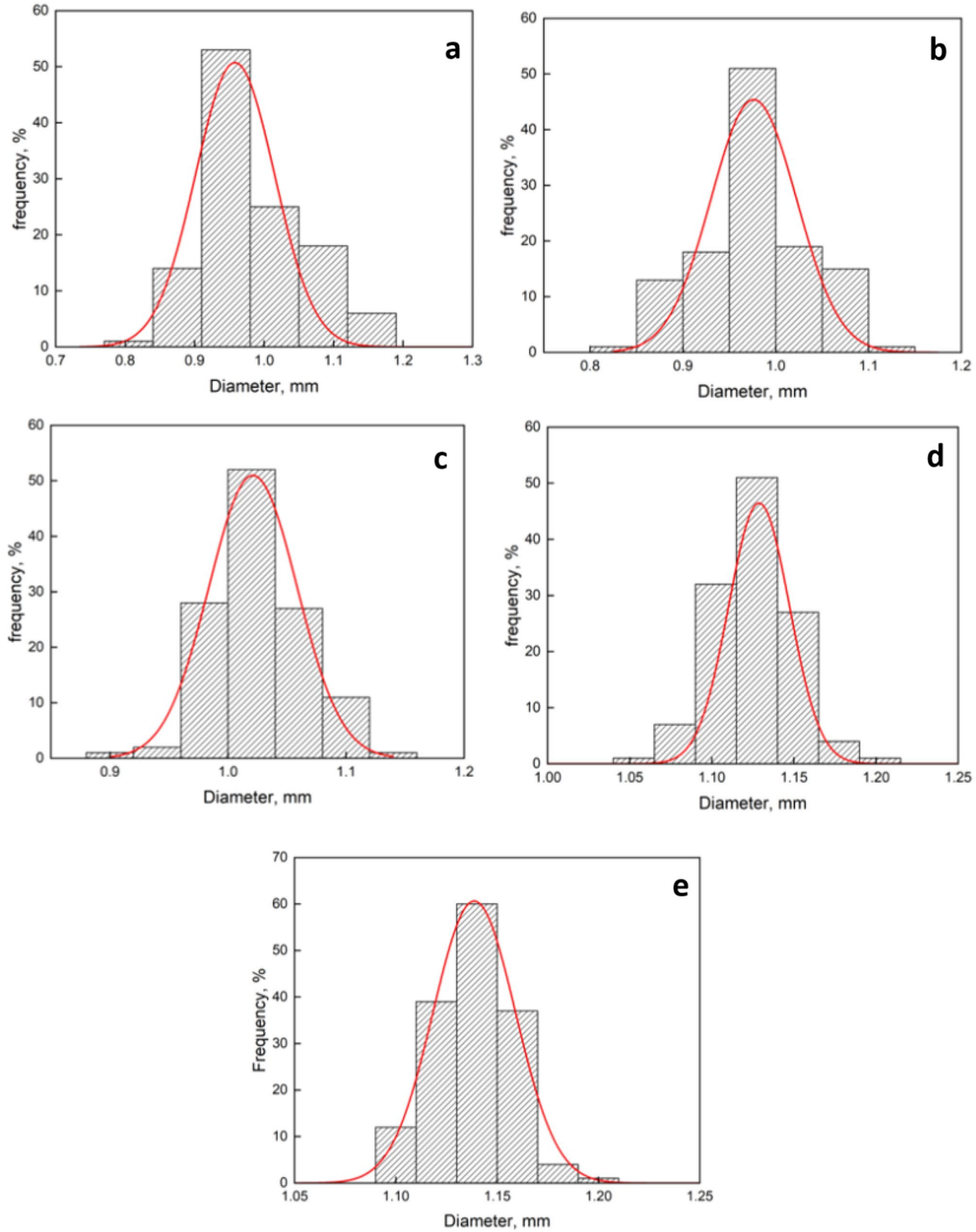

Fig. 2 Diameter distributions of **a** gelatin beads; **b** Ge–Eu beads; **c** Ge–Eu-HH 1% beads; **d** Ge–Eu-HH 3% beads and **e** Ge–Eu-HH 5% beads

Table 2 Gelatin beads diameters

Sample	Diameter, mm
Ge	0.95 ± 0.06
Ge–Eu	0.97 ± 0.05
Ge–Eu-HH 1%	1.02 ± 0.04
Ge–Eu-HH 3%	1.13 ± 0.12
Ge–Eu-HH 5%	1.15 ± 0.10

The obtained result are listed in Table 1.

Result and Discussion

Beads Diameter Distribution

Figure 2 reports the beads diameter distributions while Table 2 reports the numerical values of such diameters.

Observing the data reported in the Table 2, it can be deduced that the diameter of gelatin beads is quite constant for all samples.

FTIR Analysis

Figure 3 shows the FTIR spectra of pure gelatin bead and Ge–Eu-HH composite beads.

For the gelatin beads, three main region are present: 1627–1632, 1532–1546, and 1235–1276 cm^{-1} assigned to amide I (C%O stretching), amide II (N–H bending and C–N stretching), and amide III (C–N and N–H groups vibrating), respectively [49]. Besides, the region 3100−2800 cm^{-1} belongs to C-H stretching of gelatin structure as well as C-H stretching modes of cellulosic components of hemp hurd (CH Stretching in aromatic methoxyl groups and methylene of cellulose and hemicellulose) [50–52]. The increase in the peak intensity at 1740 cm−1, 1454 cm^{-1} and 1240 cm^{-1} could be attributed to the carbonyl (C=O) stretching vibration of the acetyl groups of hemicellulose present in the hemp hurd, CH_2 bending vibrations in lignin and to C-O stretching of acetyl [52–54]. Eugenol showed characteristic peaks at 1514, 1608 and 1637 cm^{-1} related to the aromatic C=C stretching [55], 2960–2930 cm^{-1}, and 2870–2860 cm^{-1} (stretching $–CH_3$ and $–CH_2–$); 1637 and 1463 cm^{-1} (bending $–CH_2–$); 1451 and 1366 cm^{-1} (bending $–CH_3$); and 672 cm^{-1} (bending C%C) [56]. Finally, the more pronounced peaks at 3076 cm^{-1}, 990 cm^{-1} and 720 cm^{-1} could be attributed to the C%C stretching, C%C-H_2 bending and CH_2 bending modes of eugenol [57]. These findings proved the effective encapsulation of eugenol in the gelatin beads.

Thermal Characterization

Figure 4 shows the change in weigth (%) as function of temperature (°C) of pure gelatin (Ge), Ge–Eu and Ge–Eu-HH composite beads.

The degradation of gelatin is mainly characterized by two thermal steps: loss of bound water (50 -150 °C) and thermal decompositon of gelatin matrix [58]. Figure 4 evidences that Ge beads start to decompose at about 240 °C. The Ge–Eu bead shows an additional thermal step (160-200 °C) related to the loss of eugenol [59, 60]. No further decomposition steps are present for Ge–Eu-HH beads since the thermal decomposition of the main component of hemp hurd (holocellulose (250-380 °C), cellulose (250-350 °C), hemicellulose (200-290 °C) and lignin (280-500 °C) [61–64]) occurred simultaneously to gelatin decomposition. Besides,

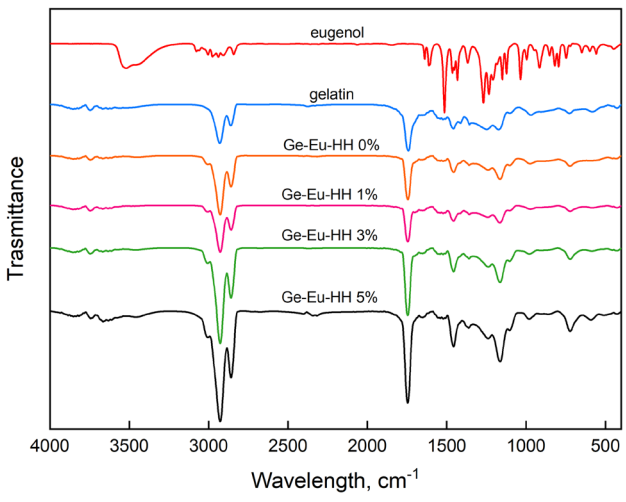

Fig. 3 FTIR spectra of pure gelatin beads, gelatin composite beads and eugenol

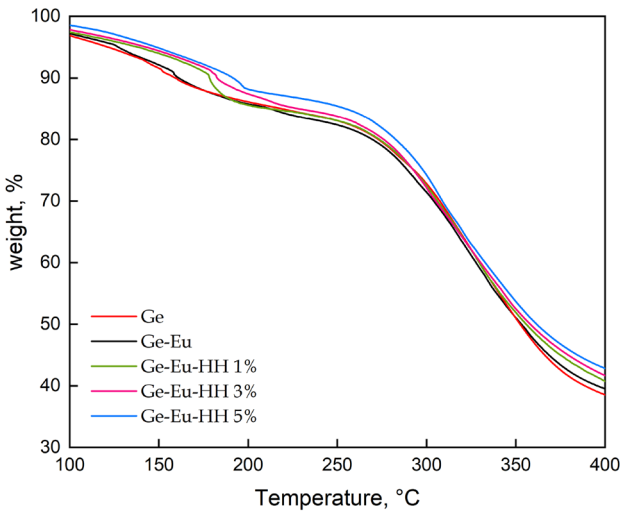

Fig. 4 Thermogravimetric curves of Ge, Ge–Eu and Ge–Eu-HH beads

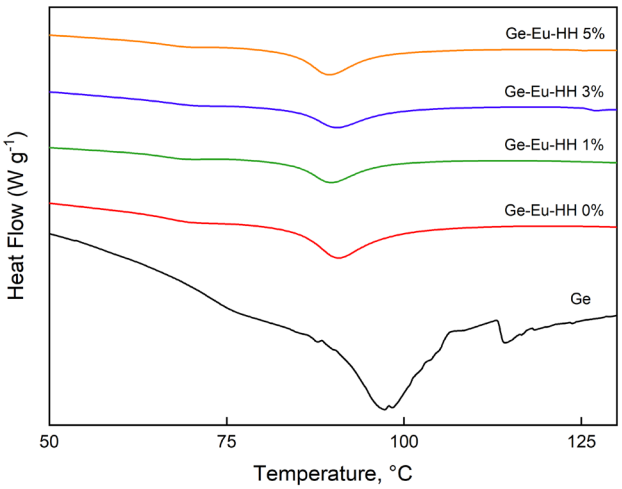

Fig. 5 DSC of neat gelatin and gelatin composite beads

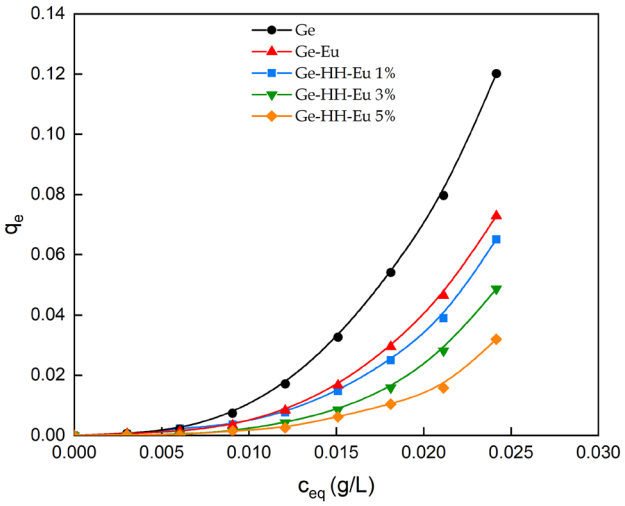

Fig. 6 Sorption isotherms of gelatin bead

Table 3 Melting temperatures of gelatin and composite gelatin beads

Sample	Melting temperature [°C]
Ge	97
Ge–Eu	90
Ge–Eu-HH 1%	89
Ge–Eu-HH 3%	88
Ge–Eu-HH 5%	89

Table 4 Sips parameters obtained by fitting experimental data with Eq. 1

Sample	q_m (g/g)	a_s (10^3 $g^n \times L^{-n}$)	n
Ge	56 ± 2.52	4.0 ± 0.10	0.36 ± 0.02
Ge–Eu	53 ± 3.66	2.8 ± 0.12	0.32 ± 0.01
Ge-HH-Eu 1%	53 ± 3.21	2.5 ± 0.13	0.31 ± 0.02
Ge-HH-Eu 3%	51 ± 2.54	2.2 ± 0.08	0.26 ± 0.03
Ge-HH-Eu 5%	40 ± 1.95	1.9 ± 0.07	0.24 ± 0.01

the onset temperature of Ge–Eu-HH-5% beads (288 °C) was delayed compared with Ge and Ge–Eu beads (about 260 °C). The thermal improvement could be attributed to hemp hurd loading. This effect might be due to the formation of hydrogen linkages involving gelatin matrix and OH groups of hemp hurd. Moreover, the formation of low molecular weight compounds, due to the thermal decomposition of hemicellulose and pectin, could generate a physical hindrance between the heat source and the polymer leading to the thermal decomposition delay. This barrier could be even responsible of the increase in mass transfer resistance for the volatile gases.

Figure 5 reports the differential thermal analysis (DSC) evaluated on gelatin beads.

In all curves, it is evident an endothermic peak related to melting temperature (T_m) [65]. The addition of hemp hurd and eugenol to beads formulation slightly altered the thermal stability of gelatin beads. The melting temperatures of all samples are reported in Table 3.

The introduction of hemp hurd powder do not alter the melting point of gelatin beads. Besides, the slight decrease in melting point of gelatin beads could be attributed to the formation of a low regular and compact chain arrangement caused by the introduction of eugenol. It follows a reduction of polymer chains movement which, in turn, allow to decrease the thermal stability of the beads [65].

Barrier Properties Evaluation

Figure 6 shows the sorption data of gelatin beads composites, reporting the equilibrium moisture content q_e (on dry basis) as a function of the water concentration C_{eq} (g/L). The knowledge of water vapor properties of hydrogel composites is required to better understand the behavior of the produced delivery systems for outdoor exposures such as agricultural ones. The improvement in hydrophobization is needed to avoid the probability of clustering occuriing or the alteration of composite properties due to the formation of cracks induced by swelling and shrinkage phenomena. The evaluation of barrier properties is crucial since a high moisture content affects dramatically the physical and chemical ageing of the composites and, thus, their lifetime in interactive environments.

The extrapolated Sips parameters from Eq. 1 are reported in Table 4:

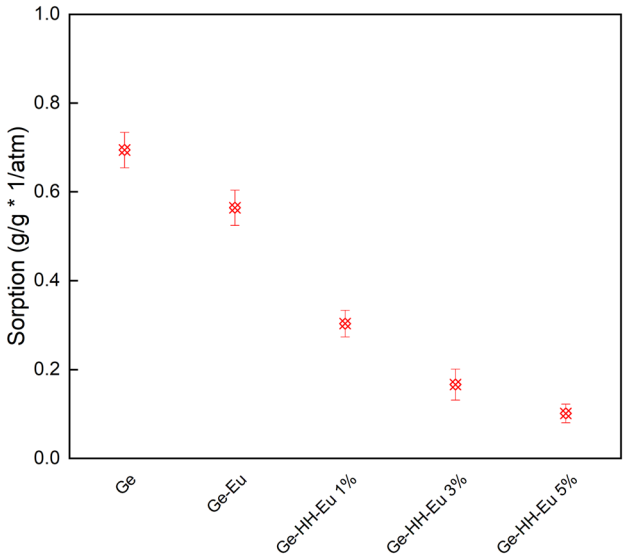

Fig. 7 Water sorption parameters of gelatin beads evaluated from Eq. 3

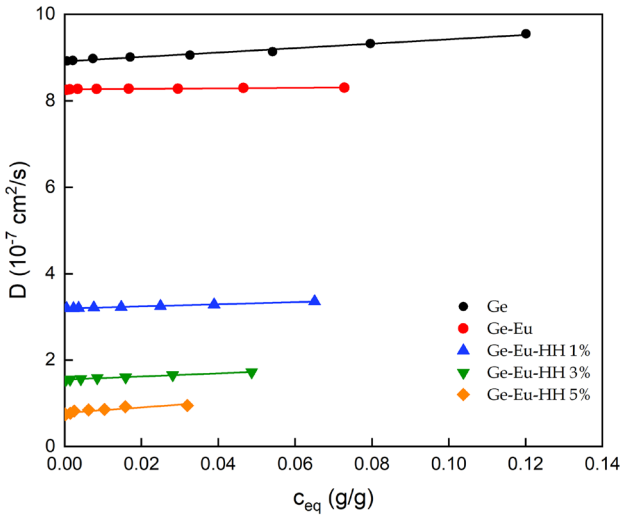

Fig. 8 Diffusion coefficient of water vapor, D (cm^2/s), as function of equilibrium moisture content Ceq (g/g)

The sorption parameters can be evaluated taking into account Henry's law of solubility (Eq. 9):

$$S = \frac{dq_e}{dP} \tag{9}$$

The sorption coefficient can be evaluated from the linear part ($0 < a_w < \cdot 0.4$) of sorption isotherm and reported in Fig. 7.

Proper interactions are supposed to occur between gelatin matrix and hemp hurd functional groups. The introduction of hemp hurd inside the gelatin matrix led to a decrease in adsorbed moisture content. Then, as evidenced in Fig. 7, as hemp hurd concentration increases, sorption parameter underwent to a substantial decrease since the hydrophobization offered by the hemp hurd components. Reduced water sorption of gelatin beads as HH amount increases can be a consequence of enhanced interaction of gelatin chain and OH groups that are less available for the interaction with water vapour. Such explanation is supported by decrease in monolayer adsorption capacity (q_m). The 1/n parameters concerns the heterogeneity of the system and, as the hemp hurd content increases, it underwent to an increase since the presence of not-homogeneous phase inside the gelatin matrix [66].

The diffusion coefficient came from the evaluation of the sorption kinetics, modeled by Fick's second law solution. The average radius reported in Table 2 was used in Fick's law solution and the diffusion coefficient has been evaluated. Figure 8 reports the log (D) as a function of the equilibrium moisture content (c_{eq}, g/g on d.b.).

Table 5 reports the D_0, the thermodynamic diffusion coefficients extrapolated at m_{eq}=0 for all the samples.

From Eq. (10) it is possible to evaluate the water permeability coefficients (reported in Table 5).

$$P = S \times D_0 \tag{10}$$

As expected and in accordance with data in Table 5, diffusivity and permeability of the composites decrease with filler loading, in full agreement with the sorption data. This could be, firstly, explained by taking into account the interactions HH-matrix, mainly hydrogen bondings, with hydrophilic groups of gelatin matrix. From transport phenomena point of view, the HH loading increases the mass transfer resistance which, likely, led to a reduction of mean cross sectional area available for water diffusion. The reduction of adsorbed water could be then attributed to the decrease in free volume due to the presence of lignocellulosic reinforcement which constituted a physical hindrance for the diffusion of water molecules, determining an higher heterogeneity of the system (as evidenced by 1/n parameter). It follows that the change in mean water molecules pathway and an increase

Table 5 D_0 and permeability coefficients

Sample	D_0 (10^{-7} cm^2/s)	P (10^{-7} g/g × 1/atm × cm^2/s)
Ge	8.91	6.15
Ge–Eu	8.26	4.63
Ge-HH-Eu 1%	3.19	0.97
Ge-HH-Eu 3%	1.55	0.26
Ge-HH-Eu 5%	0.77	0.08

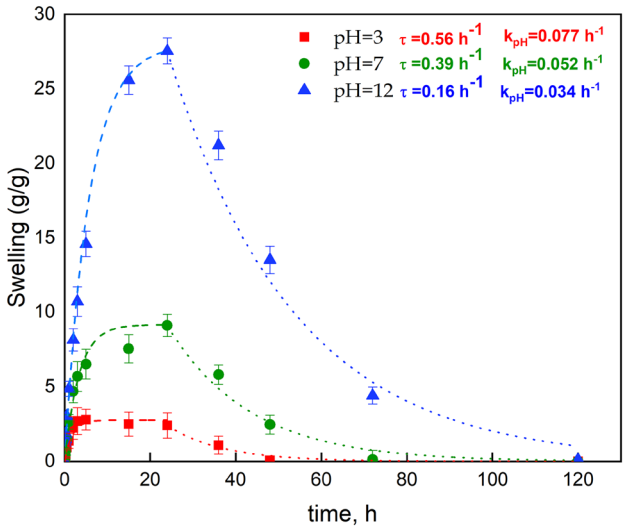

Fig. 9 Swelling and deswelling degrees of Ge beads as function of time at different pH values

in the tortuosity of the system occurred, justifying the reduction of D_0 coefficients observed.

Swelling and Deswelling Behavior

In agricultural applications, the pH has to be considered as a crucial factor to affect the release phenomena [67]. So, a deep study of the effect of pH on swelling and deswelling degree has been accomplished. Figure 9 reports swelling and deswelling degrees of gelatin beads along the time as a function of pH level.

Figure 9 highlighs the pH-dependence of swelling and deswelling behavior of gelatin beads. For short times, the rate of water uptake sharply increases and then reachs a level off. After a certain time interval, dissolution phenomena occurr and deswelling is verified. It can be deduced that gelatin swelling and deswelling degrees are clearly affected by pH of the medium due to the presence of ionizable groups [68, 69]. In acidic conditions, NH_3^+ and COOH are present while in basic conditions the species present are NH_2 and COO^-. In neutral conditions, the predominant species are NH_2/COOH [70]. It is reported that gelatin hydrogels swelled less when placed in acidic dissolution medium (pH 3) compared to other media (pH 7 and pH 12) [71, 72]. Since pKa value of main amino-acids of gelatin (glycine, proline and hydroxyproline) are 9.6, 10.6 and 10.6, as pH of medium is 12, a deprotonation of gelatin and an increase in charge on proteins is supposed to occurr. The subsequent charge repulsion of deprotonated groups lead to a higher swelling degree [73]. It follows that the ionization of all COO^- groups in gelatin increases the swelling degree of the gelatin beads. Ionic repulsion between charged groups incorporated in the gelatin matrix could be assumed to be the main driving force responsible for the swelling behaviour. As pH changes, due to the ionizable groups in gelatin chains, there are hydrostatic repulsion between them so, as gelatin beads adsorb water molecules, these latter occupy a certain volume and, as a consequence, an expansion of the structure occurrs [74]. Besides, the higher swelling at basic pH could be ascribed to the possibility of forming a porous structure due to alkaline hydrolysis [46].

Figure 9 reports the plotted experimental data according to Eqs. 3 and 4. Medium dashed lines represent the fitting curves. Rate constant values were reported in the same graph. Since τ could be considered a measure of the resistance to water permeation, lower τ value corresponds to higher water uptake rate. From Fig. 9 it is evident that after about 24 h a decrease in swelling degree can be observed due to the dissolution rate of gelatin. The dissolution of a solid in a liquid regards the transfer of mass from the solid phase to the liquid one [75]. Its rate tend to decrease as pH increases from 3 to 12, following an exponential behaviour. In acidic conditions, gelatin began to break down since the dissociation of the gelatin macromolecular structure. This phenomenon could explain the fast complete dissolution of gelation. The reported results are quite in agreement with other studies on crosslinked gelatin beads [76], polyacrylamide-gelatin [74], cross-linked acrylic acid/gelatin hydrogels [77], gelatin-based nanospheres [78] and gelatin-sodium carboxymethyl cellulose [79].

The k_{pH} constant could be considered as an estimation of the dissolution rate constant and noticeably decreases passing from acidic to basic medium as pH level differs from isoelectric point (IP) of gelatin (pH 4.7) [80]. The slowdown of gelatin beads dissolution at high pH level could be due to the inherent pH-solubility behavior of gelatin and appears to be a consequence of the physico-chemical properties of gelatin [81]. At low pH (pH <%IP), the conformation of the gelatin is probably less stable, and its overall net charge is highly positive. It follows that in the gel state, gelatin retains part of its secondary and tertiary structures and the gel rigidity decreases due to the decreased conformation stability. The dissolution of gelatin in water is quite fast and the complete bead erosion occurred in a short time interval.

Release Kinetic Evaluation: Effect of pH

The release of eugenol from gelatin composites was followed. The effect of pH on the release kinetics and the contribution of hemp hurd on the release phenomena were analyzed. The release of encapsulated compound is enabled by entry of release fluids through the systems toward the bulk and thereby the counter diffusion movement of molecules to surface of the system followed by the complete release from the polymeric system. Figure 10 report the release curves of

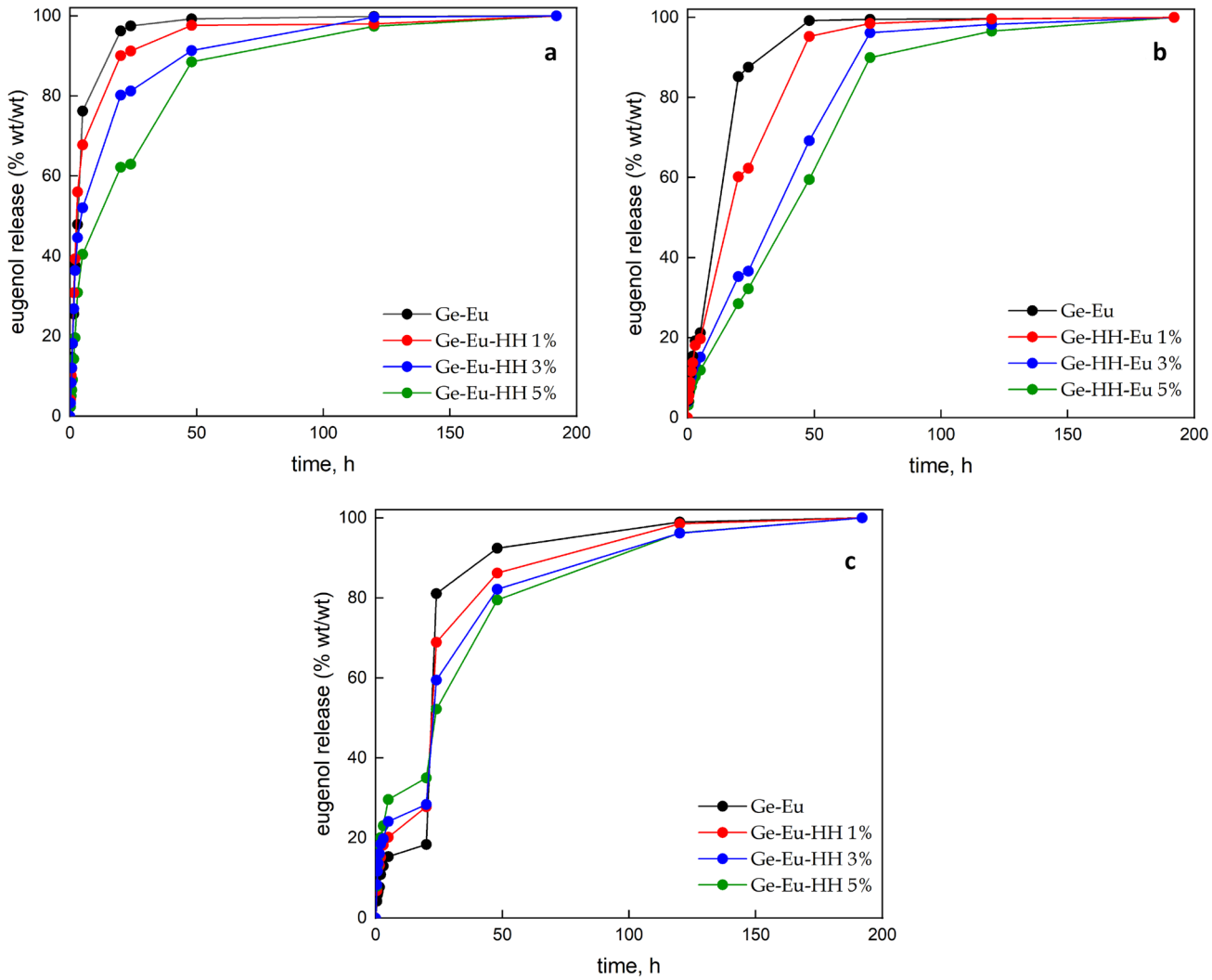

Fig. 10 Eugenol release kinetics of gelatin beads in different release media at **a** pH 3; **b** pH 7 and **c** pH 12

eugenol for pure gelatin and gelatin beads composites varying the pH of the release medium.

The mechanism and kinetics of drug releases were affected by many parameters such as physical properties of polymers, drug to polymer ratio and geometric shape of release matrix, as well as swelling and dissolution phenomena [82]. So, a complex heterogenous release curves were obtained. Figure 10 shows that the release rate of eugenol is dependent on the pH of the release medium. The initial burst release is supposed to be related to the amount of encapsulated compound not effectively protected by the carrier. It occurred since the initial swelling of the matrix and the osmotic pressure difference between the release medium and the bead [83]. The penetrating water molecules could initially generates phenomena such as relaxation of polymer chains and hydration [84]. The adsorbed water molecules could then enhance the internal pressure allowing the eugenol to be released and promoting the burst release effect. Moreover, it is worth noting that the burst is reduced as pH increases, as consequence of the higher stability of gelatin network which, probably, is able to better retain the encapsulated eugenol; then a slower and more controlled release follows [85]. As shown in Fig. 10, after 24 h more than 98% of eugenol is released from gelatin beads at pH 3. Besides, 91%, 81 and 63% of eugenol is released after 24 h for gelatin beads with 1%, 3 and 5% of hemp hurd, respectively. As pH level increases, a noticeable change of release kinetic is observed. The released eugenol after 24 h is 87%, 62%, 37 and 32 wt% (pH 7) and 81%, 68%, 60 and 52 wt% (pH 12) for Ge–Eu and gelatin beads with 1%, 3 and 5% of hemp hurd, respectively. At low pH (pH <%IP), the SD is quite reduced, as previously reported. The low stability of gelatin conformation determined a low gel rigidity, consequently the diffusion of eugenol in the release medium speeded up.

As pH >%IP, the gelatin structure is more stable and the beads are able to better adsorb water molecules determining an increase in SD. The adsorption of high amount of water and the increasing of gelatin volume could justify the higher amount of eugenol released at pH 12 compared to pH 7 conditions. In any case, the network structure due to hemp hurd located inside gelatin matrix could slow down the release rate of encapsulated eugenol. Probably, hemp hurd acts as a physical barrier which improves the mass transfer resistance by increasing the tortuosity of the system.

The fitting process of release kinetic curves allowed to obtain the k' and k'' parameters, by using Eqs. 7 and 8, which are reported in Table 1:

In controlled release formulation, swelling, diffusion and erosion represent the most important rate-controlling mechanisms. The modified Baker and Lonsdale model allowed to take into consideration all of them. The fitting of experimental release data by applying Eqs. 7 and 8 allows to evaluate the diffusion constants (k' and k'') to support the previous reported statements. The k' diffusion constant underwent a decrease as pH level increases and, for each pH regime, it decreases as hemp hurd concentrations increases. The decrease in k' constant as pH increases could be attributed to different swelling behavior of gelatin beads. Moreover, since k' constant is directly proportional to diffusion coefficient, its reduction as HH concentration increases may be due to increase in mass transfer resistance offered by HH powder which enhances the tortuosity of gelatin path length. Besides, the same behavior characterized the k'' constant which refers to dissolution regime. As gelatin bead volume decreases, due to erosion phenomena, the eugenol diffusion is favored. Moreover, a slow deswelling rate, by virtue of a slow erosion kinetic (k_{pH} constant), could partially delay the dissolution of gelatin bead external layer in conjunction with the effect of a gelatin-OH groups network which is supposed to partly put the dissolution phenomena back, in accordance with what was previously reported. Moreover, since the rate of dissolution is proportional to surface area, at relatively long experimental times, it slows down the release kinetics allowing to prolong the eugenol diffusion up to 120 h. Results confirmed that the addition of hemp hurd could lead to a decrease in eugenol released amount. The hydrophobicity of hemp hurd, due to the presence of external non cellulosic material, could enhance the reduction of water uptake rate and, as a consequence, the amount of swelling of the composite beads [86]. The mass transfer resistance generated by hemp hurd could explain the slower eugenol release rate as HH concentration increases. Finally, it could be claimed that a novel agricultural compound delivery system, completely based on renewable resources, has been designed to achive a pH-triggered release. Similar systems have already been reported in literature. Roy et al. developed calcium-alginate microspheres for controlled release of endosulfan [87] and alginate-gelatin swellable beads loaded with cypermethrin [88], reporting similar results and similar trends as pH changes. Moreover, the unique developed release system, made of aqueous gelatin/lignocellulosic material solution, is completely sustainable and no other similar systems have already been reported.

Conclusions

In this study pH-responsive composites hemp hurd/gelatin beads were produced through gelation on oil. Eugenol, a green pesticide, was encapsulated. Spectroscopic analysis confirmed the presence of eugenol and hemp hurd. Besides, thermal properties were not affected by the inclusion of hemp hurd and eugenol. Barrier properties resulted dependent on hemp hurd concentration which hydrophobicity noticeably reduced the adsorbed water content. Swelling and dissolution phenomena were studied over time (up to 8 days) and demonstrated a different behavior of gelatin beads varying the pH level of the medium. Swelling phenomenon is reduced in acidic conditions while gelatin dissolution rate was slower at basic pH compared to neutral and acidic ones. The release kinetics of eugenol was dependent on of hemp hurd and pH. Besides, even the inclusion of hemp hurd, at fixed pH level, allowed to tailor the controlled release system due to the physical hindrance of hemp hurd and the weak interaction with bound water molecules which reduced the dissolution rate. Finally, the results demonstrated the possibility of tailoring the release of a loaded compound by designing natural polymeric devices through an environmentally friendly methodology.

Acknowledgements Project Prin 2017 "MultIFunctional poLymer cOmposites based on groWn matERials (MIFLOWER)" (grant number: 2017B7MMJ5_001) from the Italian Ministry of University and Research.

Author Contributions Conceptualization: GG; formal analysis and investigation: GV; original draft preparation: GV; writing - review and editing: GV and GG; funding acquisition: GG.

Funding Open access funding provided by Università degli Studi di Salerno within the CRUI-CARE Agreement.

Declarations

Conflict of interest The authors declare no conflict of interest.

References

1. Mfarrej MFB, Rara FM (2019) Competitive, sustainable natural pesticides. Acta Ecol Sin 39:145–151. https://doi.org/10.1016/j.chnaes.2018.08.005
2. Sharma A, Shukla A, Attri K et al (2020) Global trends in pesticides: a looming threat and viable alternatives. Ecotoxicol Environ Saf 201:110812
3. Silva V, Mol HGJ, Zomer P et al (2019) Pesticide residues in European agricultural soils: a hidden reality unfolded. Sci Total Environ 653:1532–1545. https://doi.org/10.1016/j.scitotenv.2018.10.441
4. Packiam M ACTA SCIENTIFIC AGRICULTURE (ISSN: 2581-365X) Green Pesticides: Eco-friendly Technology for Integrated Pest Management
5. Wolff MS, Britton JA, Teitelbaum SL et al (2005) Improving organochlorine biomarker models for cancer research. Cancer Epidemiol Biomark Prev 14:2224–2236. https://doi.org/10.1158/1055-9965.EPI-05-0173
6. Genuis SJ, Lane K, Birkholz D (2016) Human elimination of organochlorine pesticides: blood, urine, and sweat study. Biomed Res Int. https://doi.org/10.1155/2016/1624643
7. Bugatti V, Vertuccio L, Zara S et al (2019) Green pesticides based on cinnamate anion incorporated in layered double hydroxides and dispersed in pectin matrix. Carbohydr Polym 209:356–362. https://doi.org/10.1016/j.carbpol.2019.01.033
8. Hiller E, Čerňanský S, Krascsenits Z, Milička J (2009) Effect of soil and sediment composition on acetochlor sorption and desorption. Environ Sci Pollut Res 16:546–554. https://doi.org/10.1007/s11356-009-0113-9
9. Miglioranza KSB, Aizpún de Moreno JE, Moreno VJ (2004) Land-based sources of marine pollution: organochlorine pesticides in stream systems. Environ Sci Pollut Res 11:227–232. https://doi.org/10.1007/BF02979630
10. Clementi M, Tiboni GM, Causin R et al (2008) Pesticides and fertility: an epidemiological study in Northeast Italy and review of the literature. Reprod Toxicol 26:13–18. https://doi.org/10.1016/j.reprotox.2008.05.062
11. Hatcher JM, Pennell KD, Miller GW (2008) Parkinson's disease and pesticides: a toxicological perspective. Trends Pharmacol Sci 29:322–329
12. Santadino M, Coviella C, Momo F (2014) Glyphosate sublethal effects on the population dynamics of the earthworm *Eisenia fetida* (savigny, 1826). Water Air Soil Pollut. https://doi.org/10.1007/s11270-014-2207-3
13. Mattei C, Dupont J, Wortham H, Quivet E (2019) Influence of pesticide concentration on their heterogeneous atmospheric degradation by ozone. Chemosphere. https://doi.org/10.1016/j.chemosphere.2019.04.082ï
14. Kole RK, Banerjee H, Bhattacharyya A (2001) Monitoring of market fish samples for endosulfan and hexachlorocyclohexane residues in and around calcutta. Environ Contam Toxicol. https://doi.org/10.1007/s00128-001-0159-y
15. Hedaoo RK, Gite VV (2014) Renewable resource-based polymeric microencapsulation of natural pesticide and its release study: an alternative green approach. RSC Adv 4:18637–18644. https://doi.org/10.1039/c4ra01558d
16. Lopez MD, Maudhuit A, Pascual-Villalobos MJ, Poncelet D (2012) Development of formulations to improve the controlled-release of linalool to be applied as an insecticide. J Agric Food Chem 60:1187–1192. https://doi.org/10.1021/jf204242x
17. Park M, Lee C, Il, Seo YJ et al (2010) Hybridization of the natural antibiotic, cinnamic acid, with layered double hydroxides (LDH) as green pesticide. Environ Sci Pollut Res 17:203–209. https://doi.org/10.1007/s11356-009-0235-0
18. Yang R, Xu T, Fan J et al (2018) Natural products-based pesticides: design, synthesis and pesticidal activities of novel fraxinellone derivatives containing N-phenylpyrazole moiety. Ind Crops Prod 117:50–57. https://doi.org/10.1016/j.indcrop.2018.02.088
19. Copping LG, Menn JJ (2000) Biopesticides: a review of their action, applications and efficacy. In: Pest Management Science. pp 651–676
20. Bai B, Xu X, Hai J et al (2019) Lauric acid-modified nitraria seed meal composite as green carrier material for pesticide controlled release. J Chem. https://doi.org/10.1155/2019/5376452
21. Roy A, Singh SK, Bajpai J, Bajpai AK (2014) Controlled pesticide release from biodegradable polymers. Cent Eur J Chem 12:453–469
22. Roy A, Singh S, Bajpai J et al (2014) Controlled pesticide release from biodegradable polymers. Springer 12:453–469. https://doi.org/10.2478/s11532-013-0405-2
23. Wang C, Ye W, Zheng Y et al (2007) Fabrication of drug-loaded biodegradable microcapsules for controlled release by combination of solvent evaporation and layer-by-layer self-assembly. Int J Pharm 338:165–173. https://doi.org/10.1016/j.ijpharm.2007.01.049
24. Selina OE, Chinarev AA, Obukhova PS et al (2008) Alginate-chitosan microspheres for the specific sorption of antibodies. Russ J Bioorg Chem 34:468–474. https://doi.org/10.1134/S1068162008040110
25. Panos I, Acosta N, Heras A (2009) New drug delivery systems based on chitosan. Curr Drug Discov Technol 5(4):333-41
26. Chang CP, Leung TK, Lin SM, Hsu CC (2006) Release properties on gelatin-gum arabic microcapsules containing camphor oil with added polystyrene. Colloids Surf B Biointerfaces 50:136–140. https://doi.org/10.1016/j.colsurfb.2006.04.008
27. Roy A, Bajpai J, Bajpai AK (2009) Dynamics of controlled release of chlorpyrifos from swelling and eroding biopolymeric microspheres of calcium alginate and starch. Carbohydr Polym 76:222–231. https://doi.org/10.1016/j.carbpol.2008.10.013
28. Cea M, Cartes P, Palma G, Mora ML (2010) Atrazine efficiency in an andisol as affected by clays and nanoclays in ethylcellulose controlled release formulations. Rev la Cienc del Suelo y Nutr Veg 10:62–77. https://doi.org/10.4067/S0718-27912010000100007
29. Pérez-Martínez JI, Morillo E, Maqueda C, Ginés JM (2001) Ethyl cellulose polymer microspheres for controlled release of norfluazon. Pest Manag Sci 57:688–694. https://doi.org/10.1002/ps.339
30. Roy A, Bajpai AK, Bajpai J (2009) Designing swellable beads of alginate and gelatin for controlled release of pesticide (cypermethrin). J Macromol Sci Part A 46:847–859. https://doi.org/10.1080/10601320903077976
31. Wang S, Ma Q, Wang R et al (2020) Preparation of sodium alginate-poly (vinyl alcohol) blend beads for base-triggered release of dinotefuran in Spodoptera litera midgut. Ecotoxicol Environ Saf 202:110935. https://doi.org/10.1016/j.ecoenv.2020.110935
32. Neri-Badang MC, Chakraborty S (2019) Carbohydrate polymers as controlled release devices for pesticides. J Carbohydr Chem 38:67–85. https://doi.org/10.1080/07328303.2019.1568449
33. Sathisaran I, Balasubramanian M (2020) Physical characterization of chitosan/gelatin-alginate composite beads for controlled release of urea. Heliyon 6:e05495. https://doi.org/10.1016/j.heliyon.2020.e05495

34. Li W, Ma Q, Bai Y et al (2018) Facile fabrication of gelatin/bentonite composite beads for tunable removal of anionic and cationic dyes. Chem Eng Res Des 134:336–346. https://doi.org/10.1016/j.cherd.2018.04.016
35. Hayeeye F, Sattar M, Chinpa W, Sirichote O (2017) Kinetics and thermodynamics of Rhodamine B adsorption by gelatin/activated carbon composite beads. Colloids Surfaces A Physicochem Eng Asp 513:259–266. https://doi.org/10.1016/j.colsurfa.2016.10.052
36. Zhang W, He C, Wei Z, Shi K (2020) Impact of hot water treated lotus leaves on interfacial and physico-mechanical of gelatin/lotus leaf composites. J Polym Environ 28:3270–3278. https://doi.org/10.1007/s10924-020-01778-9
37. Baygar T (2019) Bioactivity potentials of biodegradable chitosan/gelatin film forming solutions combined with monoterpenoid compounds. J Polym Environ 27:1686–1692. https://doi.org/10.1007/s10924-019-01465-4
38. Pirsa S, Farshchi E, Roufegarinejad L (2020) Antioxidant/antimicrobial film based on carboxymethyl cellulose/gelatin/tio2–ag nano-composite. J Polym Environ 28:3154–3163. https://doi.org/10.1007/s10924-020-01846-0
39. Satyanarayana KG, Arizaga GGC, Wypych F (2009) Biodegradable composites based on lignocellulosic fibers-An overview. Prog Polym Sci 34:982–1021
40. Pereira PHF, De Freitas Rosa M, Cioffi MOH et al (2015) Vegetal fibers in polymeric composites: A review. Polimeros 25:9–22
41. Bhoopathi R, Ramesh M (2020) Influence of eggshell nanoparticles and effect of alkalization on characterization of industrial hemp fibre reinforced epoxy composites. J Polym Environ 28:2178–2190. https://doi.org/10.1007/s10924-020-01756-1
42. Senthilkumar K, Ungtrakul T, Chandrasekar M et al (2020) Performance of sisal/hemp bio-based epoxy composites under accelerated weathering. J Polym Environ. https://doi.org/10.1007/s10924-020-01904-7
43. Song Y, Liu J, Chen S et al (2013) Mechanical properties of poly (lactic acid)/hemp fiber composites prepared with a novel method. J Polym Environ 21:1117–1127. https://doi.org/10.1007/s10924-013-0569-z
44. Sips R (1948) On the structure of a catalyst surface. Phys Adsorpt Non-Uniform Surf J Chem Phys 16:931. https://doi.org/10.1063/1.1746922
45. Jeppu GP, Clement TP (2012) A modified Langmuir--Freundlich isotherm model for simulating pH-dependent adsorption effects. J Contam Hydrol 129–130:46–53. https://doi.org/10.1016/j.jconhyd.2011.12.001
46. Omidian H, Hashemi SA, Sammes PG, Meldrum I (1998) A model for the swelling of superabsorbent polymers. Polymer 39:6697–6704. https://doi.org/10.1016/S0032-3861(98)00095-0
47. Rani S, Sharma AK, Khan I et al (2017) Polymeric nanoparticles in targeting and delivery of drugs. Nanotechnology-based approaches for targeting and delivery of drugs and genes. Elsevier, Amsterdam, pp 223–255
48. Chien YW (1988) Controlled release of biologically active agents. J Pharm Sci 77:371. https://doi.org/10.1002/jps.2600770422
49. Rawdkuen S, Faseha A, Benjakul S, Kaewprachu P (2020) Application of anthocyanin as a color indicator in gelatin films. Food Biosci 36:100603. https://doi.org/10.1016/j.fbio.2020.100603
50. Arsyanti L, Erwanto, Rohman A, Pranoto Y (2018) Chemical composition and characterization of skin gelatin from buffalo (Bubalus bubalis)
51. Viscusi G, Barra G, Gorrasi G (2020) Modification of hemp fibers through alkaline attack assisted by mechanical milling: effect of processing time on the morphology of the system. Cellulose 27:8653–8665. https://doi.org/10.1007/s10570-020-03406-0
52. Terpáková E, Kidalová L, Eštoková A et al (2012) Chemical modification of hemp shives and their characterization. Procedia Engineering. Elsevier, Amsterdam, pp 931–941
53. Rachini A, Le Troedec M, Peyratout C, Smith A (2009) Comparison of the thermal degradation of natural, alkali-treated and silane-treated hemp fibers under air and an inert atmosphere. J Appl Polym Sci 112:226–234. https://doi.org/10.1002/app.29412
54. Sawpan MA, Pickering KL, Fernyhough A (2011) Effect of various chemical treatments on the fibre structure and tensile properties of industrial hemp fibres. Compos Part A Appl Sci Manuf 42:888–895. https://doi.org/10.1016/j.compositesa.2011.03.008
55. Li Y, Dong Q, Chen J, Li L (2020) Effects of coaxial electrospun eugenol loaded core-sheath PVP/shellac fibrous films on postharvest quality and shelf life of strawberries. Postharvest Biol Technol 159:111028. https://doi.org/10.1016/j.postharvbio.2019.111028
56. Bonilla J, Poloni T, Lourenço RV, Sobral PJA (2018) Antioxidant potential of eugenol and ginger essential oils with gelatin/chitosan films. Food Biosci 23:107–114. https://doi.org/10.1016/j.fbio.2018.03.007
57. Dhoot G, Auras R, Rubino M et al (2009) Determination of eugenol diffusion through LLDPE using FTIR-ATR flow cell and HPLC techniques. Polymer 50:1470–1482. https://doi.org/10.1016/j.polymer.2009.01.026
58. Mishra RK, Majeed ABA, Banthia AK (2011) Development and characterization of pectin/gelatin hydrogel membranes for wound dressing. Int J Plast Technol 15:82–95. https://doi.org/10.1007/s12588-011-9016-y
59. Celebioglu A, Irem Yildiz Z, Uyar T (2017) Fabrication of electrospun eugenol/cyclodextrin inclusion complex nanofibrous webs for enhanced antioxidant property, water solubility, and high temperature stability. ACS Publ 66:457–466. https://doi.org/10.1021/acs.jafc.7b04312
60. Kayaci F, Ertas Y, Uyar T (2013) Enhanced thermal stability of eugenol by cyclodextrin inclusion complex encapsulated in electrospun polymeric nanofibers. ACS Publ 61:8156–8165. https://doi.org/10.1021/jf402923c
61. Stevulova N, Cigasova J, Purcz P, Schwarzova I (2014) Long-term water absorption behaviour of hemp hurds composites. Chem Eng Trans 39:559–564. https://doi.org/10.3303/CET1439094
62. Fisher T, Hajaligol M, Waymack B, Kellogg D (2002) Pyrolysis behavior and kinetics of biomass derived materials. J Anal Appl Pyrolysis 62:331–349. https://doi.org/10.1016/S0165-2370(01)00129-2
63. Kabir MM, Wang H, Lau KT, Cardona F (2013) Effects of chemical treatments on hemp fibre structure. Appl Surf Sci 276:13–23. https://doi.org/10.1016/j.apsusc.2013.02.086
64. Sebio-Puñal T, Naya S, López-Beceiro J et al (2012) Thermogravimetric analysis of wood, holocellulose, and lignin from five wood species. In: Journal of Thermal Analysis and Calorimetry. pp 1163–1167
65. Sahraee S, Milani JM, Ghanbarzadeh B, Hamishehkar H (2017) Physicochemical and antifungal properties of bio-nanocomposite film based on gelatin-chitin nanoparticles. Int J Biol Macromol 97:373–381. https://doi.org/10.1016/j.ijbiomac.2016.12.066
66. Mohammadi Nafchi A, Moradpour M, Saeidi M, Alias AK (2014) Effects of nanorod-rich ZnO on rheological, sorption isotherm, and physicochemical properties of bovine gelatin films. LWT - Food Sci Technol 58:142–149. https://doi.org/10.1016/j.lwt.2014.03.007
67. Roy A, Bajpai AK, Bajpai J (2009) Designing swellable beads of alginate and gelatin for controlled release of pesticide (cypermethrin) designing swellable beads of alginate and gelatin for controlled release of pesticide (cypermethrin). J Macromol Sci A. https://doi.org/10.1080/10601320903077976

68. Gordon PW, Brooker ADM, Chew YMJ et al (2010) Studies into the swelling of gelatine films using a scanning fluid dynamic gauge. Food Bioprod Process 88:357–364. https://doi.org/10.1016/j.fbp.2010.08.012
69. Kalaleh H-A, Tally M, Atassi Y (2015) Preparation of poly(sodium acrylate-co-acrylamide) superabsorbent copolymer via alkaline hydrolysis of acrylamide using microwave irradiation
70. Pourjavadi A, Mahdaviniag R (2006) Superabsorbency, pH-sensitivity and swelling kinetics of partially hydrolyzed chitosan-g-poly(acrylamide) hydrogels. Turk J Chem 30:5
71. Oliveira GF, Ferrari PC, Carvalho LQ, Evangelista RC (2010) Chitosan-pectin multiparticulate systems associated with enteric polymers for colonic drug delivery. Carbohydr Polym 82:1004–1009. https://doi.org/10.1016/j.carbpol.2010.06.041
72. Wang S, Shao G, Yang J et al (2020) The production of gel beads of soybean hull polysaccharides loaded with soy isoflavone and their pH-dependent release. Food Chem 313:126095. https://doi.org/10.1016/j.foodchem.2019.126095
73. Yang XJ, Zheng PJ, Cui ZD et al (1997) Swelling behaviour and elastic properties of gelatin gels. Polym Int 44:448–452
74. Martínez-Ruvalcaba A, Becerra-Bracamontes F, Sánchez-Díaz JC, González-Álvarez A (2009) Polyacrylamide-gelatin polymeric networks: effect of pH and gelatin concentration on the swelling kinetics and mechanical properties. Polym Bull 62:539–548. https://doi.org/10.1007/s00289-008-0037-4
75. GVP, CHRISTOPER MPP (2018) Release kinetics: concepts and applications. Int J Pharm Res Technol 8:12–20
76. Qiao C, Cao X, Wang F (2012) Swelling behavior study of physically crosslinked gelatin hydrogels. Polym Polym Compos 20:53–58. https://doi.org/10.1177/096739111202001-210
77. Bukhari SMH, Khan S, Rehanullah M, Ranjha NM (2015) Synthesis and characterization of chemically cross-linked acrylic acid/gelatin hydrogels: effect of pH and composition on swelling and drug release. Int J Polym Sci. https://doi.org/10.1155/2015/187961
78. Curcio M, Altimari I, Spizzirri UG et al (2013) Biodegradable gelatin-based nanospheres as pH-responsive drug delivery systems. J Nanopart Res 15:1–11. https://doi.org/10.1007/s11051-013-1581-x
79. Rathna GVN, Mohan Rao DV, Chatterji PR (1996) Hydrogels of gelatin-sodium carboxymethyl cellulose: synthesis and swelling kinetics. J Macromol Sci 33:1199–1207. https://doi.org/10.1080/10601329608010914
80. Xiao L, Yu ZY, Yang C et al (2004) Swelling studies of chitosan-gelatin films cross-linked by sulfate. Wuhan Univ J Nat Sci 9:247–251. https://doi.org/10.1007/bf02830611
81. Zhao F, Malayev V, Rao V, Hussain M (2004) Effect of sodium lauryl sulfate in dissolution media on dissolution of hard gelatin capsule shells. Pharm Res 21:144–148. https://doi.org/10.1023/B:PHAM.0000012162.52419.b3
82. Ainurofiq A, Choiri S (2015) Drug release model and kinetics of natural polymers-based sustained release tablet. Lat Am J Pharm 37:1328–1337
83. Saber-Samandari S, Saber-Samandari S, Joneidi-Yekta H, Mohseni M (2017) Adsorption of anionic and cationic dyes from aqueous solution using gelatin-based magnetic nanocomposite beads comprising carboxylic acid functionalized carbon nanotube. Chem Eng J 308:1133–1144. https://doi.org/10.1016/j.cej.2016.10.017
84. Ford JL, Rubinstein MH, McCaul F et al (1987) Importance of drug type, tablet shape and added diluents on drug release kinetics from hydroxypropylmethylcellulose matrix tablets. Int J Pharm 40:223–234. https://doi.org/10.1016/0378-5173(87)90172-4
85. Gallagher KM, Corrigan OI (2000) Mechanistic aspects of the release of levamisole hydrochloride from biodegradable polymers. J Control Release 69:261–272. https://doi.org/10.1016/S0168-3659(00)00305-9
86. Saber-Samandari S, Saber-Samandari S, Gazi M (2013) Cellulose-graft-polyacrylamide/hydroxyapatite composite hydrogel with possible application in removal of Cu (II) ions. React Funct Polym 73:1523–1530. https://doi.org/10.1016/j.reactfunctpolym.2013.07.007
87. Roy A, Bajpai J, Bajpai AK (2009) Development of calcium alginate-gelatin based microspheres for controlled release of endosulfan as a model pesticide. Indian J Chem Technol 16:388–395
88. Roy A, Bajpai AK, Bajpai J (2009) Designing swellable beads of alginate and gelatin for controlled release of pesticide (cypermethrin). J Macromol Sci Part A 46:847–859. https://doi.org/10.1080/10601320903077976